Decays $B \to D_{(s)}^{(*)} h$ $(h = \pi, \rho)$ in a confined covariant quark model

S. Dubnička,[1] A. Z. Dubničková,[2] M. A. Ivanov,[3] and A. Liptaj[1,*]

[1]*Institute of Physics, Slovak Academy of Sciences, 845 11 Bratislava, Slovak Republic*
[2]*Department of Theoretical Physics, Faculty of Mathematics, Physics and Informatics, Comenius University, 842 48 Bratislava, Slovak Republic*
[3]*Bogoliubov Laboratory of Theoretical Physics, Joint Institute for Nuclear Research, 141980 Dubna, Russia*

(Received 17 June 2022; accepted 3 August 2022; published 26 August 2022)

Decay processes $B \to D_{(s)}^{(*)} h$ $(h = \pi, \rho)$ are studied in the framework of the confined covariant quark model using the naïve factorization assumption. We observe that the theoretical results on branching fractions have a tendency to systematically exceed the experimental numbers. Such a behavior has already been seen for similar processes by other authors.

DOI: 10.1103/PhysRevD.106.033006

I. INTRODUCTION

The recent measurements by the Belle [1] and LHCb [2] Collaborations complement the previous *BABAR* results [3–5] on B decays into D particles and pions. Including also reactions with the ϱ meson in the final state [5–8], we focus in this analysis on a set of decay processes with a rich mix of properties. The processes differ in spin and flavor structure and are described by various diagram topologies. Rather than addressing some specific question, we see several broader motivations for our study. First, we are interested in the ability of the confined covariant quark model (CCQM) to describe the experimental branching fraction values as established from the new measurements. The importance of their good theoretical understanding stems from the fact that several of the studied decay channels have a clean experimental signature measured with a high statistical significance and thus play an important role of a relative reference for processes, which are more difficult to measure. Further, in the framework we use, we rely on the naïve factorization assumption, which we in this way also indirectly test. The assumption is presumed valid for the processes with the spectator quark entering the D meson, which is justified in the heavy-quark limit [9]. The latter can be no longer upheld if the spectator quark becomes part of the light meson. In addition, our description of the chosen processes depends on five CKM matrix elements, i.e., on all except V_{us} and those related to the top quark. So, our ability to describe various decay processes within a single framework can be also seen as a probe and a consistency check of the weak sector understanding. Finally, our previous works covered most of the interesting nonleptonic $B_{(c,s)}$ decays [10–14]. B decays to light unflavored mesons and D particles were within the CCQM not treated up to now.

In Sec. II we review the description of the selected decays in the Standard Model a provide formulas for amplitudes and decay widths. In Sec. III the main features of the CCQM are discussed and hadronic form factors are computed. In the last section we present results and conclude the text.

II. AMPLITUDES AND DECAY WIDTHS

B mesons can decay only weakly via the internal W exchange. Two-body decays have three different quark topologies shown in Fig. 1.

The annihilation topology is not taken into account since its contribution can be neglected (see Sec. 3.3.6 of [9]).

The weak decays are described in the effective theory approach based on a Hamiltonian constructed from four-fermion operators Q_i weighted by scale-dependent Wilson coefficients $C_i(\mu)$ and CKM factors V_i

$$\mathcal{H}_{\text{eff}} = -\frac{G_F}{\sqrt{2}} \sum V_i C_i(\mu) Q_i,$$

where G_F is the Fermi constant and $V_i = V_{q_1,q_2} V^{\dagger}_{q_3,q_4}$. At leading order two operators play a role,

*andrej.liptaj@savba.sk

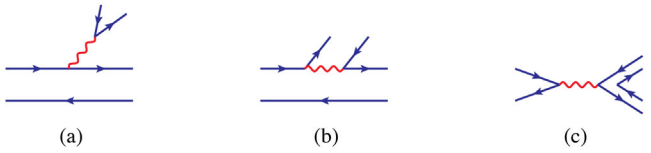

FIG. 1. Quark diagrams with three different topologies: color favored (a), color suppressed (b), and annihilation (c).

$$Q_1 = ((\overline{q_1})_{i_1}(q_2)_{i_2})_{V-A}((\overline{q_3})_{i_2}(q_4)_{i_1})_{V-A},$$
$$Q_2 = ((\overline{q_1})_{i_1}(q_2)_{i_1})_{V-A}((\overline{q_3})_{i_2}(q_4)_{i_2})_{V-A},$$
$$(\bar{q}_1 q_2)_{V-A} \equiv \bar{q}_1 O^\mu q_2 = \bar{q}_1 \gamma^\mu (1-\gamma^5) q_2,$$

where $i_{1,2}$ are color indices and q represents quark fields.

The calculation of the matrix elements describing the nonleptonic decays of the B meson into $D_{(s)}^{(*)}$ and light mesons $\pi(\rho)$ proceeds in our CCQM by analogy with the decays of the B_c meson into charmonium and $D(D_s)$ meson (for great details, see Ref. [10]). A pictorial representation of the matrix elements is shown in Fig. 2. By using the Fierz transformations one can show that diagram (b) with color-suppressed topology is equal to diagram (a) times the prefactor $\xi = 1/N_c$. This corresponds to the so-called factorization hypothesis. Therefore, the combinations of the Wilson coefficients appear as $a_1 = C_2 + \xi C_1$ and $a_2 = C_1 + \xi C_2$. In the numerical calculations we set the color-suppressed parameter ξ to zero. Then one has

$$a_1 = C_2 = 1.0111, \quad \text{and} \quad a_2 = C_1 = -0.2632. \quad (1)$$

We take values of the Wilson coefficients from [15], where they were computed at the matching scale $\mu_0 = 2M_W$ at the NNLO precision and run down to the hadronic scale $\mu_b = 4.8$ GeV.

Due to the above-mentioned factorization, the matrix elements of two-body nonleptonic decays split into leptonic weak decay of the one daughter meson and weak transition of the B meson into another daughter meson. The leptonic weak decays are characterized by the weak leptonic decay constants which have been reliably calculated in our previous papers.

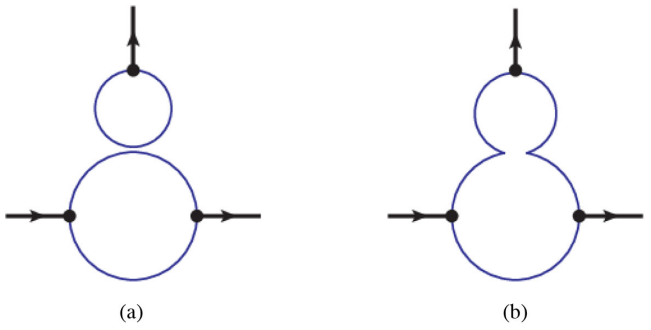

FIG. 2. Pictorial representation of the matrix elements of the nonleptonic B decays with color-favored (a) and color-suppressed (b) topologies.

The matrix elements of the $B \to H$ transition can be described with help of covariant form factors where the form of the parametrization depends on the spin of H. For pseudoscalar particles ($H = PS$) and vector particles ($H = V$) one has

$$\langle PS_{[\bar{q}_3,q_2]}(p_H)|\bar{q}_1 O^\mu q_2|B_{[\bar{q}_3,q_1]}(p_b)\rangle = F_+(q^2)P^\mu + F_-(q^2)q^\mu,$$
$$\langle V_{[\bar{q}_3,q_2]}(p_H,\epsilon)|\bar{q}_1 O^\mu q_2|B_{[\bar{q}_3,q_1]}(p_b)\rangle = \frac{\epsilon_\nu^\dagger}{m_H+m_V}[-g_{\mu\nu}P\cdot qA_0(q^2) + P^\mu P^\nu A_+(q^2) + q^\mu P^\nu A_-(q^2) + i\varepsilon^{\mu\nu\alpha\beta}P_\alpha q_\beta V(q^2)].$$

Here the momenta $P = p_B + p_H$ and $q = p_B - p_H$ are the sum and the difference of the ingoing and outgoing momenta, respectively. Because operators $Q_{1,2}$ do not contain $\sigma^{\mu\nu}q_\nu$ terms, the corresponding tensor form factors do not enter our analysis. It is convenient to define helicity form factors

(i) $B \to PS$

$$H_t = \frac{1}{\sqrt{q^2}}[(m_B^2 - m_H^2)F_+ + q^2 F_-],$$
$$H_0 = \frac{2m_B|\mathbf{p_2}|}{\sqrt{q^2}}F_+,$$

(ii) $B \to V$

$$H_t = \frac{1}{m_B+m_H}\frac{m_B|\mathbf{p_2}|}{m_H\sqrt{q^2}} \times [(m_B^2 - m_H^2)(A_+ - A_0) + q^2 A_-],$$
$$H_\pm = \frac{1}{m_B+m_H}[-(m_B^2 - m_H^2)A_0 \pm 2m_B|\mathbf{p_2}|V],$$
$$H_0 = \frac{1}{m_B+m_H}[-(m_B^2 - m_H^2)(m_B^2 - m_H^2 - q^2)A_0 + 4m_B^2|\mathbf{p_2}|^2 A_+],$$

with $|\mathbf{p_2}| = \sqrt{\lambda^{\text{Källen}}(m_B^2, m_H^2, m_{H'}^2)}/2m_B$ being the momentum of the final state particles H and H' in the rest frame of B.

The decay width formula depends on the diagram topology and spin structure. The studied processes can be organized in Table I in the following way. The diagram D_1 describes the contribution proportional to the Wilson coefficient a_1, the diagram D_2 describes the contribution proportional to the Wilson coefficient a_2, and the diagram

TABLE I. Classification of processes.

	Diagram type		
Spin structure	D_1	D_2	D_3
(A) $\underline{\boldsymbol{PS \to PS}} + PS$	$\underline{B^0 \to D^-} + \pi^+$ $\underline{B^0 \to \pi^-} + D^+$ $\underline{B^0 \to \pi^-} + D_s^+$ $\underline{B^+ \to \pi^0} + D_s^+$	$\underline{B^0 \to \pi^0} + \bar{D}^0$	$\underline{B^+ \to \bar{D}^0} + \pi^+$
(B) $\underline{\boldsymbol{PS \to PS}} + V$	$\underline{B^0 \to D^-} + \varrho^+$ $\underline{B^0 \to \pi^-} + D_s^{*+}$ $\underline{B^+ \to \pi^0} + D^{*+}$ $\underline{B^+ \to \pi^0} + D_s^{*+}$	$\underline{B^0 \to \pi^0} + \overline{D^{*0}}$	$\underline{B^+ \to \bar{D}^0} + \varrho^+$
(C) $\underline{\boldsymbol{PS \to V}} + PS$	$\underline{B^0 \to D^{*-}} + \pi^+$ $\underline{B^0 \to \varrho^-} + D_s^+$ $\underline{B^+ \to \varrho^0} + D_s^+$	$\underline{B^0 \to \varrho^0} + \bar{D}^0$	$\underline{B^+ \to \overline{D^{*0}}} + \pi^+$
(D) $\underline{\boldsymbol{PS \to V}} + V$	$\underline{B^0 \to D^{*-}} + \varrho^+$ $\underline{B^0 \to \varrho^-} + D_s^{*+}$ $\underline{B^+ \to \varrho^0} + D_s^{*+}$	$\underline{B^0 \to \varrho^0} + \overline{D^{*0}}$	$\underline{B^+ \to \overline{D^{*0}}} + \varrho^+$

D_3 describes the contribution proportional to the mixture of a_1 and a_2. Such diagram types are depicted in Fig. 3.

For the processes listed in Table I we underline the part containing the transition of the spectator quark, for the D_3 case we apply this rule to the first of the two diagrams. The $D_{1/2/3}$ decays are sometimes referred to as class-$1/2/3$ processes [16], D_2 are called color suppressed. In our analysis we do not distinguish between u and d quarks and denote both by q. In order to make the decay width formulas compact we introduce the symbol θ_0 which takes the value $1/\sqrt{2}$ if an unflavored light neutral meson is in the final state and is equal to one otherwise. The formulas for the D_1 decays are

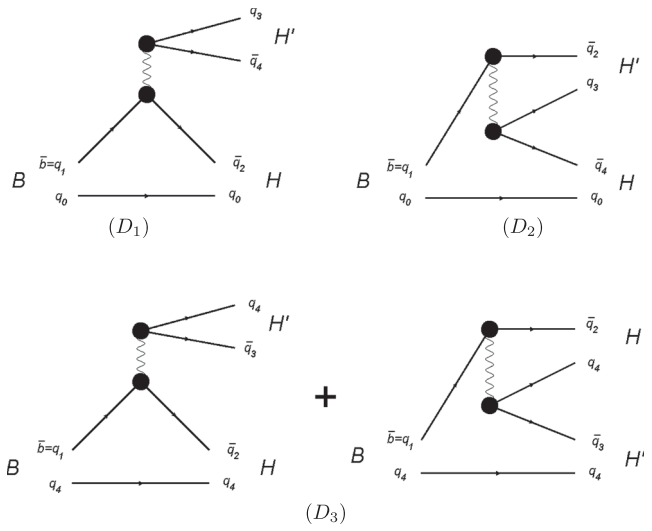

FIG. 3. Diagram structures D_1, D_2, and D_3.

$$\Gamma_{[A,D_1]}(\underline{S_1 \to S_2} + S_3) = \frac{G_F^2}{16\pi}\frac{|\boldsymbol{p}_2|}{m_{S_1}^2}|\theta_0 V_{q_1q_2}V_{q_3q_4}^\dagger a_1 f_{S_3} m_{S_3}|^2 \times \{H_t^{S_1\to S_2}(m_{S_3}^2)\}^2,$$

$$\Gamma_{[B,D_1]}(\underline{S_1 \to S_2} + V) = \frac{G_F^2}{16\pi}\frac{|\boldsymbol{p}_2|}{m_{S_1}^2}|\theta_0 V_{q_1q_2}V_{q_3q_4}^\dagger a_1 f_V m_V|^2 \times \{H_0^{S_1\to S_2}(m_V^2)\}^2,$$

$$\Gamma_{[C,D_1]}(\underline{S_1 \to V} + S_2) = \frac{G_F^2}{16\pi}\frac{|\boldsymbol{p}_2|}{m_{S_1}^2}|\theta_0 V_{q_1q_2}V_{q_3q_4}^\dagger a_1 f_{S_2} m_{S_2}|^2 \times \{H_t^{S_1\to V}(m_{S_2}^2)\}^2,$$

$$\Gamma_{[D,D_1]}(\underline{S \to V_1} + V_2) = \frac{G_F^2}{16\pi}\frac{|\boldsymbol{p}_2|}{m_S^2}|\theta_0 V_{q_1q_2}V_{q_3q_4}^\dagger a_1 f_{V_2} m_{V_2}|^2 \times \sum_{i=0,\pm}\{H_i^{S_1\to V_1}(m_{V_2}^2)\}^2.$$

The decay formulas for the color-suppressed D_2 processes can be written as a function of those for D_1:

$$\Gamma_{[X,D_2]}^{[a_1,a_2]}(\underline{B \to H} + H') = \Gamma_{[X,D_1]}^{[a_2,a_1]}(\underline{B \to H} + H'),$$

where the roles of the a_1 and a_2 coefficients are swapped. The decay widths of the D_3 processes are given by

$$\Gamma_{[A,D_3]}(\underline{S_1 \to S_2} + S_3) = \frac{G_F^2}{16\pi}\frac{|\boldsymbol{p}_2|}{m_{S_1}^2}\theta_0^2|V_{q_1q_2}V_{q_3q_4}^\dagger|^2 \times \{a_1 f_{S_3} m_{S_3} H_t^{S_1\to S_2}(m_{S_3}^2) + a_2 f_{S_2} m_{S_2} H_t^{S_1\to S_3}(m_{S_2}^2)\}^2,$$

$$\Gamma_{[B,D_3]}(\underline{S_1 \to S_2} + V) = \frac{G_F^2}{16\pi}\frac{|\boldsymbol{p}_2|}{m_{S_1}^2}\theta_0^2|V_{q_1q_2}V_{q_3q_4}^\dagger|^2 \times \{a_1 f_V m_V H_0^{S_1\to S_2}(m_V^2) + a_2 f_{S_2} m_{S_2} H_t^{S_1\to V}(m_{S_2}^2)\}^2,$$

$$\Gamma_{[C,D_3]}(\underline{S_1 \to V} + S_2) = \frac{G_F^2}{16\pi}\frac{|\boldsymbol{p}_2|}{m_{S_1}^2}\theta_0^2|V_{q_1q_2}V_{q_3q_4}^\dagger|^2 \times \{a_1 f_{S_2} m_{S_2} H_t^{S_1\to V}(m_{S_2}^2) + a_2 f_V m_V H_0^{S_1\to S_2}(m_V^2)\}^2,$$

$$\Gamma_{[D,D_3]}(\underline{S \to V_1} + V_2) = \frac{G_F^2}{16\pi}\frac{|\boldsymbol{p}_2|}{m_S^2}\theta_0^2|V_{q_1q_2}V_{q_3q_4}^\dagger|^2 \times \sum_{i=0,\pm}\{a_1 f_{V_2} m_{V_2} H_i^{S\to V_1}(m_{V_2}^2) + a_2 f_{V_1} m_{V_1} H_i^{S\to V_2}(m_{V_1}^2)\}^2.$$

The last ingredient necessary for the evaluation of decay widths are the hadronic form factors. Because of their nonperturbative nature, one has to rely on a

model-dependent approach. We evaluate these form factors within the CCQM.

III. HADRONIC FORM FACTORS IN CCQM

The description of nonleptonic heavy meson decays in the framework of the CCQM was already presented several times [10–14,17]. We summarize here the most important attributes of our approach.

The CCQM uses the scheme where a hadron is before the interaction converted into its constituent quarks. This is expressed by the nonlocal effective Lagrangian

$$\mathcal{L}_{\rm int} = g_M M(x) J_M(x) + \text{H.c.},$$
$$J_M(x) = \int dx_1 \int dx_2 F_M(x; x_1, x_2) \bar{q}_2(x_2) \Gamma_M q_1(x_1),$$

which guarantees a full Lorentz covariance. The interaction strength between the mesonic field M and its interpolating quark current J_M is given by the coupling g_M. The current is constructed from quark fields q, an appropriate Dirac matrix Γ_M, and a vertex function F_M. The latter is chosen to have a translational invariant form

$$F_M(x; x_1, x_2) = \delta(x - w_1 x_1 - w_2 x_2) \Phi_M[(x_1 - x_2)^2]$$

with $w_i = m_{q_i}/(m_{q_1} + m_{q_2})$, so that the meson position x can be interpreted as the barycenter of the quark system. The function Φ_M is taken Gaussian in the momentum representation

$$\Phi_M[(x_1 - x_2)^2] = \int \frac{d^4k}{(2\pi)^4} e^{-ik(x_1 - x_2)} \tilde{\Phi}_M(-k^2),$$
$$\tilde{\Phi}_M(-k^2) = e^{k^2/\Lambda_M^2}.$$

Here Λ_M is a free parameter of the model which characterizes the meson M.

The presence of both hadrons and quarks raises concerns about the double counting. We remedy the latter by applying the so-called compositeness condition [18]

$$Z_M = 1 - g_M^2 \Pi_M'(m_M^2) = 0, \tag{2}$$

which originates in the works [19–21]. Here Π_M' is the derivative of the mass operator corresponding to the self–energy diagram of the meson field fluctuating into a pair of quarks. Setting the renormalization constant $Z_M^{1/2}$ to zero implies that the physical and the corresponding bare state have no overlap, i.e., the physical state does not contain the bare state and is therefore interpreted as bound. The condition effectively excludes the constituent degrees of freedom from the space of physical states because the constituents exist in virtual states only. The equality in (2) is reached by an appropriate choice of g_M and in this way the coupling constants are determined and do not appear as model parameters.

Another notable feature of the CCQM is the confining property. So as to prevent hadrons from decaying into quarks in situations where the hadron mass is greater than those of constituent quarks summed, an infrared cutoff $1/\lambda^2$

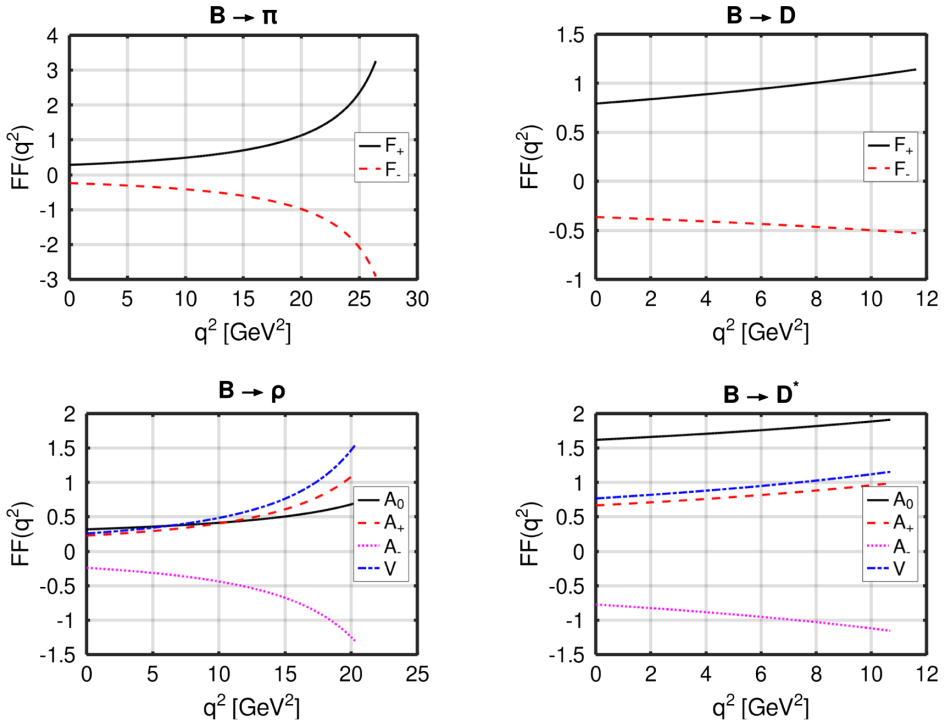

FIG. 4. Form factors of transitions which determine the investigated decays.

TABLE II. CCQM parameters. Values are in GeV.

Λ_B	Λ_D	Λ_{D^*}	Λ_{D_s}	$\Lambda_{D_s^*}$	Λ_π	Λ_ρ	m_b	m_s	m_q	λ
1.96	1.60	1.53	1.75	1.56	0.87	0.61	5.04	0.428	0.241	0.181

is introduced as an upper integration limit in the integration over the space of Schwinger parameters. The latter appear in the parametrization of quark propagators, which become, after the cutoff being applied, entire functions with all possible thresholds in the corresponding quark loop diagrams removed (more details given in [22], Sec. II C).

The evaluation of hadronic form factors within the CCQM proceeds via standard computation techniques based on evaluation of the corresponding Feynman diagrams. For the $B \to PS$ and $B \to V$ transition the form factors are given by

$$
\begin{aligned}
&F_+(q^2)P^\mu + F_-(q^2)q^\mu \\
&\quad = \frac{3g_B g_H}{4\pi^2}\int \frac{d^4k}{4\pi^2 i}\tilde{\Phi}_B[-(k+w_b p_B)^2]\tilde{\Phi}_H[-(k+w_{q_i}p_H)^2] \\
&\qquad \times \mathrm{Tr}[S_{q_i}(k+p_H)O^\mu S_b(k+p_B)\gamma^5 S_{q_s}(k)\gamma^5], \\
&\frac{\epsilon^*_{H\nu}}{m_B+m_H}[-g^{\mu\nu}Pq A_0(q^2) + P^\mu P^\nu A_+(q^2) \\
&\qquad + q^\mu P^\nu A_-(q^2) + i\varepsilon^{\mu\nu\alpha\beta}P_\alpha q_\beta V(q^2)] \\
&\quad = \frac{3g_B g_H}{4\pi^2}\int \frac{d^4k}{4\pi^2 i}\tilde{\Phi}_B[-(k+w_b p_B)^2]\tilde{\Phi}_H[-(k+w_{q_i}p_H)^2] \\
&\qquad \times \mathrm{Tr}[S_{q_i}(k+p_H)O^\mu S_b(k+p_B)\gamma^5 S_{q_s}(k)\,\epsilon_{H\mu}\gamma^\mu].
\end{aligned}
$$

Here q_s and q_i denote the spectator and the interacting quark of H, respectively (H being PS or V), S represents quark propagators and ϵ_H the polarization vector of $H \equiv V$. Giving the vertex functions the above-mentioned Gaussian form and writing the propagators in the Schwinger representation, one performs the loop integration and applies the infrared cutoff in the integration over the Schwinger parameters, this last integration being done numerically. The model parameters were determined in our previous works [18,23] and their numerical values are shown in Table II. The predicted behavior of form factors in four studied transitions is shown in Fig. 4.

IV. RESULTS, CONCLUSION

Our results are summarized in Table III. All model parameters have been fixed using a χ^2 fit to data (leptonic decay constants, variuos coupling constants, etc.), taking into account their experimental uncertainties. By propagating these, we estimate the errors of our parameters to be at the level of 10% which then translates as a 20% error of our results.

The precision of the description of the experimental data is limited, as seen in Fig. 5. The central values of the

TABLE III. Computed branching fractions compared with experimental measurements [24].

	Process	Diagram	$\mathcal{B}_{\mathrm{CCQM}}$/E	$\mathcal{B}_{\mathrm{PDG}}$/E	E
1	$B^0 \to D^- + \pi^+$	D_1	5.34 ± 1.07	2.52 ± 0.13	10^{-3}
2	$B^0 \to \pi^- + D^+$	D_1	11.19 ± 2.24	7.4 ± 1.3	10^{-7}
3	$B^0 \to \pi^- + D_s^+$	D_1	3.48 ± 0.70	2.16 ± 0.26	10^{-5}
4	$B^+ \to \pi^0 + D_s^+$	D_1	1.88 ± 0.38	1.6 ± 0.5	10^{-5}
5	$B^0 \to D^- + \rho^+$	D_1	14.06 ± 2.81	7.6 ± 1.2	10^{-3}
6	$B^0 \to \pi^- + D_s^{*+}$	D_1	3.66 ± 0.73	2.1 ± 0.4	10^{-5}
7	$B^+ \to \pi^0 + D^{*+}$	D_1	0.804 ± 0.16	<3.6	10^{-6}
8	$B^+ \to \pi^0 + D_s^{*+}$	D_1	0.197 ± 0.04	<2.6	10^{-4}
9	$B^0 \to D^{*-} + \pi^+$	D_1	4.74 ± 0.95	2.74 ± 0.13	10^{-3}
10	$B^0 \to \rho^- + D_s^+$	D_1	2.76 ± 0.55	<2.4	10^{-5}
11	$B^+ \to \rho^0 + D_s^+$	D_1	0.149 ± 0.03	<3.0	10^{-4}
12	$B^0 \to D^{*-} + \rho^+$	D_1	14.58 ± 2.92	6.8 ± 0.9	10^{-3}
13	$B^0 \to \rho^- + D_s^{*+}$	D_1	5.09 ± 1.02	4.1 ± 1.3	10^{-5}
14	$B^+ \to \rho^0 + D_s^{*+}$	D_1	0.275 ± 0.06	<4.0	10^{-4}
15	$B^0 \to \pi^0 + \bar{D}^0$	D_2	0.085 ± 0.02	2.63 ± 0.14	10^{-4}
16	$B^0 \to \pi^0 + \bar{D}^{*0}$	D_2	1.13 ± 0.23	2.2 ± 0.6	10^{-4}
17	$B^0 \to \rho^0 + \bar{D}^0$	D_2	0.675 ± 0.14	3.21 ± 0.21	10^{-4}
18	$B^0 \to \rho^0 + \bar{D}^{*0}$	D_2	1.50 ± 0.30	<5.1	10^{-4}
19	$B^+ \to \bar{D}^0 + \pi^+$	D_3	3.89 ± 0.78	4.68 ± 0.13	10^{-3}
20	$B^+ \to \bar{D}^0 + \rho^+$	D_3	1.83 ± 0.37	1.34 ± 0.18	10^{-2}
21	$B^+ \to \bar{D}^{*0} + \pi^+$	D_3	7.60 ± 1.52	4.9 ± 0.17	10^{-3}
22	$B^+ \to \bar{D}^{*0} + \rho^+$	D_3	11.75 ± 2.35	9.8 ± 1.7	10^{-3}

CCQM numbers are in agreement with those measurements which provide upper limits and in two other cases they lay inside 1σ error of the measured value. For the rest, the CCQM provides mostly fair estimates of the experimental numbers, usually within the factor of 2. However, also in these situations the difference in terms of standard

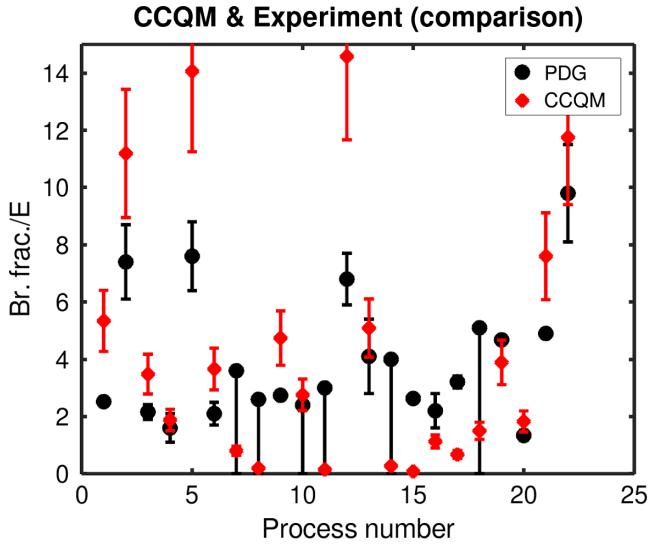

FIG. 5. CCQM branching fraction predictions compared with the experimental values listed in the PDG [24]. Processes are numbered as in Table III.

deviations can be large, if the measured point has a small error. From this point of view large deviations are seen for color-suppressed processes[1] (15)(17) and for those with $B \to D^{(*)}$ transition (1)(9)(21). Since the factorization assumption has no solid justification for the color-suppressed decays we address, we attribute the observed difference in (15)(17) to its breaking. Concerning processes (1)(9)(21), they have rather small experimental errors which may partly explain the large differences in terms of sigmas. One may also notice that they share the same set of form factors which implies correlation in their behavior and one indeed observes important overestimation also for other $B \to D^{(*)}$ processes, e.g., (5)(12). Actually, an overestimation is seen for almost all D_1 and D_3 decays [with the exception of (19)], the overestimation is just more pronounced for some processes than for others. Such a systematic shift is somewhat surprising, but we are not the first to observe it, see [25,26]. The authors of [27] notice the same behavior in similar decays too. They argue that it is difficult to provide a solid explanation within the Standard Model and thus propose new physics mechanisms. Our results seem to confirm their observations, which they label as a "novel puzzle." New physics explanations are also investigated in [28]. The comparison of our results with those of other authors is shown in Table IV.

[1]We use process numbers as in Table III.

TABLE IV. Comparison of theoretical predictions for chosen branching fractions (in units 10^{-3}).

Decay mode	Our results	[25]	[28]
$B^0 \to D^- \pi^+$	5.34 ± 1.07	$3.93^{+0.43}_{-0.42}$	$4.74^{+0.61}_{-0.69}$
$B^0 \to D^{*-} \pi^+$	4.74 ± 0.95	$3.45^{+0.53}_{-0.50}$	$4.26^{+0.75}_{-0.80}$
$B^0 \to D^- \rho^+$	14.06 ± 2.81	$10.42^{+1.24}_{-1.20}$	$12.28^{+1.40}_{-1.63}$
$B^0 \to D^{*-} \rho^+$	14.58 ± 2.92	$9.24^{+0.72}_{-0.71}$	$11.61^{+1.88}_{-2.01}$

ACKNOWLEDGMENTS

S. D., A. Z. D., and A. L. acknowledge the support from the Scientific Grant Agency VEGA, Grant No. 2/0105/21. All authors acknowledge the support from the Joint Research Project of the Institute of Physics, Slovak Academy of Sciences and the Bogoliubov Laboratory of Theoretical Physics, Joint Institute for Nuclear Research, Grant No. 01-3-1135-2019/2023.

[1] E. Waheed *et al.*, Study of $\bar{B}^0 \to D^+ h^- (h = K/\pi)$ decays at Belle, Phys. Rev. D **105**, 012003 (2021).
[2] Roel Aaij *et al.*, Measurement of the branching fraction of the $B^0 \to D_s^+ \pi^-$ decay, Eur. Phys. J. C **81**, 314 (2021).
[3] Bernard Aubert *et al.*, Evidence for the Rare Decay $B^+ \to D_s^+ \pi^0$, Phys. Rev. Lett. **98**, 171801 (2007).
[4] Bernard Aubert *et al.*, Branching fraction measurement of $B^0 \to D^{(*)} + \pi^-$, $B^- \to D^{(*)0} \pi^-$ and isospin analysis of $\bar{B} \to D^{(*)} \pi$ decays, Phys. Rev. D **75**, 031101 (2007).
[5] Bernard Aubert *et al.*, Measurement of the absolute branching fractions $B \to D_\pi, D_\pi^*, D_\pi^{**}$ with a missing mass method, Phys. Rev. D **74**, 111102 (2006).
[6] Roel Aaij *et al.*, Dalitz plot analysis of $B^0 \to \bar{D}^0 \pi^+ \pi^-$ decays, Phys. Rev. D **92**, 032002 (2015).
[7] S. E. Csorna *et al.*, Measurements of the branching fractions and helicity amplitudes in $B \to D^* \rho$ decays, Phys. Rev. D **67**, 112002 (2003).
[8] M. S. Alam *et al.*, Exclusive hadronic B decays to charm and charmonium final states, Phys. Rev. D **50**, 43 (1994).
[9] M. Beneke, G. Buchalla, M. Neubert, and Christopher T. Sachrajda, QCD factorization for exclusive, nonleptonic B meson decays: General arguments and the case of heavy light final states, Nucl. Phys. **B591**, 313 (2000).
[10] Stanislav Dubnicka, Anna Z. Dubnickova, Aidos Issadykov, Mikhail A. Ivanov, and Andrej Liptaj, Study of B_c decays into charmonia and D mesons, Phys. Rev. D **96**, 076017 (2017).
[11] Stanislav Dubnicka, Anna Z. Dubnickova, Mikhail A. Ivanov, and Andrej Liptaj, Decays $B_s \to J/\psi + \eta$ and $B_s \to J/\psi + \eta'$ in the framework of covariant quark model, Phys. Rev. D **87**, 074021 (2013).
[12] Mikhail A. Ivanov, Jurgen G. Körner, Sergey G. Kovalenko, Pietro Santorelli, and Gozyal G. Saidullaeva, Form factors for semileptonic, nonleptonic and rare $B(B_s)$ meson decays, Phys. Rev. D **85**, 034004 (2012).
[13] Michail A. Ivanov, J. G. Körner, and O. N. Pakhomova, The Nonleptonic decays $B_c^+ \to D_s^+ \bar{D}^0$ and $B_c^+ \to D_s^+ D^0$ in a relativistic quark model, Phys. Lett. B **555**, 189 (2003).
[14] Mikhail A. Ivanov, Jurgen G. Körner, and Pietro Santorelli, Exclusive semileptonic and nonleptonic decays of the B_c meson, Phys. Rev. D **73**, 054024 (2006).
[15] Sebastien Descotes-Genon, Tobias Hurth, Joaquim Matias, and Javier Virto, Optimizing the basis of $B \to K^* ll$ observables in the full kinematic range, J. High Energy Phys. 05 (2013) 137.
[16] Matthias Neubert and Alexey A. Petrov, Comments on color suppressed hadronic B decays, Phys. Lett. B **519**, 50 (2001).
[17] Georges Aad *et al.*, Study of $B_c^+ \to J/\psi D_s^+$ and $B_c^+ \to J/\psi D_s^{*+}$ decays in pp collisions at $\sqrt{s} = 13$ TeV with the ATLAS detector, J. High Energy Phys. 08 (2022) 087.
[18] Gurjav Ganbold, Thomas Gutsche, Mikhail A. Ivanov, and Valery E. Lyubovitskij, On the meson mass spectrum in the covariant confined quark model, J. Phys. G **42**, 075002 (2015).

[19] B. Jouvet, On the meaning of Fermi coupling, Nuovo Cimento **3**, 1133 (1956).
[20] Abdus Salam, Lagrangian theory of composite particles, Nuovo Cimento **25**, 224 (1962).
[21] Steven Weinberg, Elementary particle theory of composite particles, Phys. Rev. **130**, 776 (1963).
[22] Tanja Branz, Amand Faessler, Thomas Gutsche, Mikhail A. Ivanov, Jurgen G. Körner, and Valery E. Lyubovitskij, Relativistic constituent quark model with infrared confinement, Phys. Rev. D **81**, 034010 (2010).
[23] Mikhail A. Ivanov, Jurgen G. Körner, and Chan T. Tran, Exclusive decays $b \to \ell^- \bar{\nu}$ and $b \to d^{(*)} \ell^- \bar{\nu}$ in the covariant quark model, Phys. Rev. D **92**, 114022 (2015).
[24] P. A. Zyla *et al.*, Review of particle physics, Prog. Theor. Exp. Phys. **2020**, 083C01 (2020).
[25] Tobias Huber, Susanne Kränkl, and Xin-Qiang Li, Two-body non-leptonic heavy-to-heavy decays at NNLO in QCD factorization, J. High Energy Phys. 09 (2016) 112.
[26] Marzia Bordone, Nico Gubernari, Tobias Huber, Martin Jung, and Danny van Dyk, A puzzle in $\bar{B}_{(s)}^0 \to D_{(s)}^{(*)+}\{\pi^-, K^-\}$ decays and extraction of the f_s/f_d fragmentation fraction, Eur. Phys. J. C **80**, 951 (2020).
[27] Syuhei Iguro and Teppei Kitahara, Implications for new physics from a novel puzzle in $\bar{B}_{(s)}^0 \to D_{(s)}^{(*)+}\{\pi^-, K^-\}$ decays, Phys. Rev. D **102**, 071701 (2020).
[28] Fang-Min Cai, Wei-Jun Deng, Xin-Qiang Li, and Ya-Dong Yang, Probing new physics in class-I B-meson decays into heavy-light final states, J. High Energy Phys. 10 (2021) 235.